Molecular Dynamics Studies of the Hydration of α,α-Trehalose

Qiang Liu,[†] R. K. Schmidt,[†,‡] B. Teo,[†] P. A. Karplus,[§] and J. W. Brady*[,†]

Contribution from the Department of Food Science, Stocking Hall, and Section of Biochemistry, Molecular and Cell Biology, Biotechnology Building, Cornell University, Ithaca, New York 14853

Received March 12, 1997. Revised Manuscript Received May 19, 1997[⊗]

Abstract: Molecular dynamics simulations have been used to model the aqueous solvation of the nonreducing sugar α,α-trehalose. The anisotropic structuring of water around the trehalose molecule was calculated in a Cartesian coordinate frame fixed with respect to the sugar molecule by averaging water positions over the trajectories and was plotted in two and three dimensions relative to the sugar. The hydrogen bonding of this sugar to solvent was calculated and compared to other sugar solutes. Hydration was required to produce the experimental conformation, through the exchange of an internal hydrogen bond for similar bonds to solvent. This equilibrium conformation was found to impose extensive structuring on the adjacent solvent, with structuring extending out to at least the third "solvation shell", while pure liquid water exhibits such structure only in its nearest neighbors. The details of the structuring are determined by both the specific stereochemical topology of the molecule and its conformation, with considerable interplay between conformation and solvent structure. The effect of solute flexibility on the application of this solvent density mapping technique was also examined. While the extensive solvent structural perturbation induced by the solute suggests why the sugars in general are useful antidessicants and cryoprotectants, trehalose does not appear from these results to be unique in its solvation properties. In addition, the results are consistent with the suggestion that much of the effectiveness of trehalose could result from its direct binding to biological membranes and proteins rather than from unique solution properties.

I. Introduction

With their large number of hydrogen-bonding hydroxyl groups, carbohydrates might be expected to interact strongly with water. In general, the solvation properties of the carbohydrates are a function of the specific stereochemical arrangement of the hydroxyl groups of each molecule, and each sugar solution will have distinct properties,[1] even for stereoisomers differing in structure at only one asymmetric carbon. The structural details of a carbohydrate can determine how it interacts with solvent water molecules in ways which are not yet completely understood. Sugars are generally thought of as net "structure-makers",[2] meaning that they impose a collective structure on the adjacent solvent different from that which it would otherwise adopt. While it is sometimes possible to characterize such solvent structuring from diffraction studies of hydrated crystals of biological molecules,[3,4] it has been much more difficult to determine the details of solvent structure in dilute liquid solutions, particularly for non-spherically-symmetric molecular solutes.[5] The consequences of such structuring, however, are quite important in determining a number of physical properties of carbohydrate solutions. Organisms exploit the water-structuring characteristics of the different sugars in a variety of ways, such as to modify the viscosity of cellular fluids and to protect against freezing or dehydration.[6,7] Determining how molecular structures affect solution properties would be of general utility in understanding biopolymer systems and could have practical applications, as in the design of novel cryoprotectants.

The trehaloses are a family of nonreducing disaccharides that result from the combination of two D-glucopyranose molecules through (1→1) glycosidic linkages. Three such dimers are possible, α,α, α,β, and β,β, indicating the linkage configurations. The α,α-trehalose dimer (Figure 1a), which hereafter will simply be referred to as "trehalose", occurs in significant amounts in certain plants, seeds, and invertebrates adapted to endure drought,[8,9] and it has been shown that this disaccharide is able to stabilize proteins and lipid bilayers *in vitro* during dehydration. Several mechanisms for the antidessicant properties of trehalose have been advanced. Trehalose solutions have the highest glass transition temperature of any of the disaccharides,[7,8,10] suggesting that the ability of trehalose to stabilize biological systems is related to its ability to control water mobility by forming a glassy state. It has also been proposed that the stabilizing effect may result from direct interactions of the disaccharide with proteins and phospholipid head groups,[11] perhaps replacing hydrogen-bonded solvent molecules.

In part because of its potential practical applications in cryobiology, trehalose has been studied extensively,[6,7,12−17] but

* Author to whom correspondence should be addressed.
† Department of Food Science.
‡ Present Address: Division of Biochemistry and Molecular Biology, John Curtin School of Medical Research, Australian National University, Canberra, ACT 0200, Australia.
§ Section of Biochemistry, Molecular and Cell Biology.
⊗ Abstract published in *Advance ACS Abstracts,* August 1, 1997.

(1) Goldberg, R. N.; Tewari, Y. B. *J. Phys. Chem. Ref. Data* **1989**, *18*, 809−880.
(2) Walrafen, G. E.; Fisher, M. R. *Methods Enzymol.* **1986**, *127*, 91−105.
(3) Karplus, P. A.; Faerman, C. *Curr. Opin. Struct. Biol.* **1994**, *4*, 770−776.
(4) Jeffrey, G. A.; Huang, D.-B. *Carbohydr. Res.* **1990**, *206*, 173−182.
(5) Soper, A. K. *J. Chem. Phys.* **1994**, *101*, 6888−6901.
(6) Koster, K. L.; Leopold, A. C. *Plant Physiol.* **1988**, *88*, 829−832.
(7) Green, J. L.; Angell, C. A. *J. Phys. Chem.* **1989**, *93*, 2880−2882.
(8) Crowe, L. M.; Reid, D. S.; Crowe, J. H. *Biophys. J.* **1996**, *71*, 2087−2093.
(9) Weisburd, S. *Sci. News* **1988**, *133*, 97−112.
(10) Ding, S.-P.; Fan, J.; Green, J. L.; Lu, Q.; Sanchez, E.; Angell, C. A. *J. Thermal Anal.* **1996**, *47*, 1391−1405.
(11) Crowe, J. H.; Crowe, L. M.; Chapman, D. *Science* **1984**, *223*, 701−703.
(12) Bock, K.; Defaye, J.; Driguez, H.; Bar-Guilloux, E. *Eur. J. Biochem.* **1983**, *131*, 595−600.
(13) Ram, P.; Mazzola, L.; Prestegard, J. H. *J. Am. Chem. Soc.* **1989**, *111*, 3176−3182.
(14) Duda, C. A.; Stevens, E. S. *J. Am. Chem. Soc.* **1990**, *112*, 7406.
(15) Gaffney, S. H.; Haslam, E.; Lilley, T. H.; Ward, T. R. *J. Chem. Soc., Faraday Trans. 1* **1988**, *84*, 2545−2552.

S0002-7863(97)00798-1 CCC: $14.00

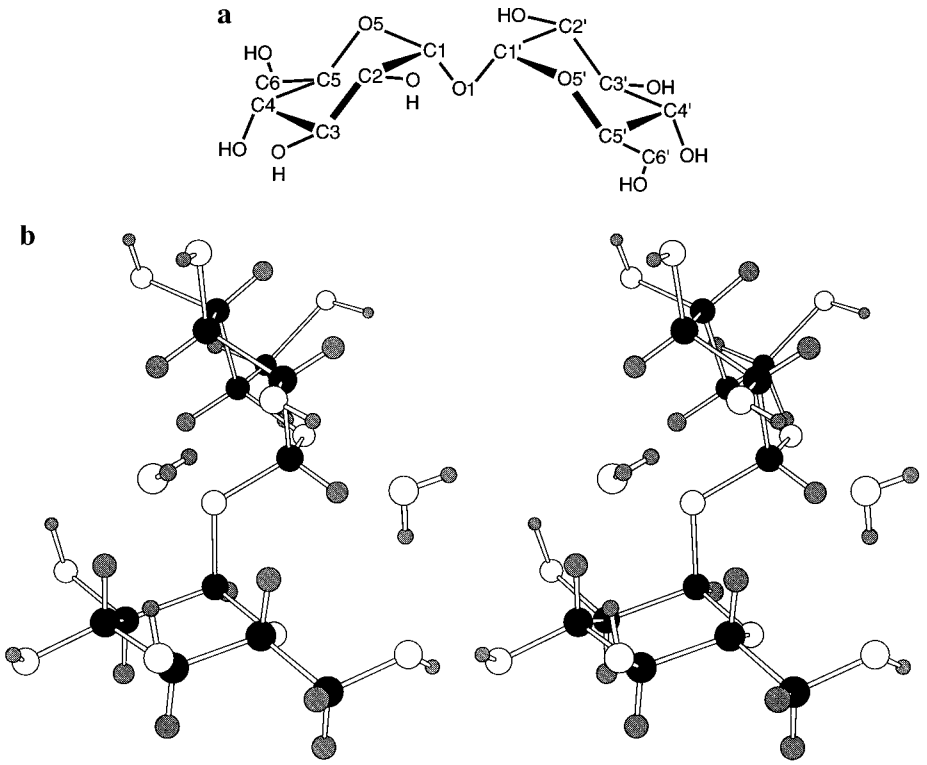

Figure 1. (a) A schematic representation of α,α-trehalose indicating the atomic numbering. (b) The crystal structure of α,α-trehalose dihydrate.[44]

some uncertainty remains about its properties in aqueous solution. Unfortunately, the conformations of disaccharides in solution have in general been difficult to characterize experimentally. NMR approaches are somewhat limited since there are no proton−proton couplings across the glycosidic linkage, $^3J_{CH}$ heteronuclear couplings are often weak and difficult to interpret, and there are generally too few NOEs across the glycosidic linkage to uniquely specify disaccharide conformations. The application of NMR to trehalose is further hampered by the symmetry of the nonisotopically-labeled molecule, with only one set of resonances for the equivalent glucose rings.[13] Recently, Batta et al.[17] have reported NOE and coupling constant data for α,α-trehalose asymmetrically ^{13}C-labeled at the C1 position, and their reported solution conformation is consistent with previous experimental estimates.[12,14]

Because of the experimental difficulties, molecular mechanics calculations have often been used to model disaccharide conformations,[18−20] as a supplement to experimental information, and such calculations have been applied to trehalose.[21,22] In addition to the difficulties encountered in determining the conformations of carbohydrates, the molecular-level details of the structure and dynamics of solvent water in carbohydrate solutions are also difficult to study experimentally, but can be readily modeled by using Monte Carlo or molecular dynamics (MD) simulations.[23,24] Such simulation techniques have been widely applied to aqueous solutions, including those of various carbohydrates.[25−30] Recently, Donnamaria et al.[31] reported MD simulations of trehalose in aqueous solution using the GROMOS molecular dynamics program[32,33] and the SPC/E water model.[34] From atomic pair correlation functions, hydrogen bond patterns, and diffusion coefficients, these authors concluded that trehalose does not significantly modify the properties of its aqueous solvent. However, these results are at variance with other simulations of carbohydrates, which have found that not only do the sugars impose extensive structure on the adjacent water, but that this structuring is important to the observed properties of the solution.[30,35] To further examine this question, this paper reports the calculation of an adiabatic, Ramachandran-like conformational energy map for trehalose and the results of new MD simulations of trehalose in vacuum and water. A procedure for mapping the average three-dimensional distribution of water molecules around the solute is described and used to examine the anisotropic structuring imposed on the solvent by trehalose. The results of the solution trajectories and the solvent density mapping are used to interpret the effects of hydration on the conformation of the disaccharide.

(16) Uedaira, H.; Ishimura, M.; Tsuda, S.; Uedaira, H. *Bull. Chem. Soc. Jpn.* **1990**, *63*, 3376−3379.
(17) Batta, G.; Kover, K. E.; Gervay, J.; Hornyak, M.; Roberts, G. M. *J. Am. Chem. Soc.* **1997**, *119*, 1336−1345.
(18) Brant, D. A. *Annu. Rev. Biophys. Bioeng.* **1972**, *1*, 369−408.
(19) Brady, J. W. *Adv. Biophys. Bioeng.* **1990**, *1*, 155−202.
(20) *Computer Modeling of Carbohydrate Molecules*; French, A. D., Brady, J. W., Eds.; American Chemical Society: Washington, DC, 1990; Vol. 430.
(21) Tvaroska, I.; Vaclavik, L. *Carbohydr. Res.* **1987**, *160*, 137−149.
(22) Dowd, M. K.; Reilly, P. J.; French, A. D. *J. Comput. Chem.* **1992**, *13*, 102−114.
(23) McCammon, J. A.; Harvey, S. C. *Dynamics of Proteins and Nucleic Acids*; Cambridge University Press: Cambridge, 1987.
(24) Brooks, C. L.; Karplus, M.; Pettitt, B. M. *Proteins: A Theoretical Perspective of Dynamics, Structure, and Thermodynamics*; Wiley-Interscience: New York, 1988; Vol. LXXI.
(25) Brady, J. W. *J. Am. Chem. Soc.* **1989**, *111*, 5155−5165.
(26) van Eijck, B. P.; Kroon, J. *J. Mol. Struct.* **1989**, *195*, 133−146.
(27) van Eijck, B. P.; Kroon-Batenburg, L. M. J.; Kroon, J. *J. Mol. Struct.* **1990**, *237*, 315−325.
(28) Brady, J. W.; Schmidt, R. K. *J. Phys. Chem.* **1993**, *97*, 958−966.
(29) Hardy, B. J.; Sarko, A. *J. Comput. Chem.* **1993**, *14*, 848−857.
(30) Schmidt, R. K.; Karplus, M.; Brady, J. W. *J. Am. Chem. Soc.* **1996**, *118*, 541−546.
(31) Donnamaria, M. C.; Howard, E. I.; Grigera, J. R. *J. Chem. Soc., Faraday Trans.* **1994**, *90*, 2731−2735.
(32) van Gunsteren, W. F.; Berendsen, H. J. C. *Groningen Molecular Simulation (GROMOS) Library Manual*; Biomos: Groningen, The Netherlands, 1987.
(33) Hermans, J.; Berendsen, H. J. C.; van Gunsteren, W. F.; Postma, J. P. M. *Biopolymers* **1984**, *23*, 1513−1518.
(34) Berendsen, H. J. C.; Grigera, J. R.; Straatsma, T. P. *J. Phys. Chem.* **1987**, *91*, 6269−6271.
(35) Liu, Q.; Brady, J. W. *J. Am. Chem. Soc.* **1996**, *118*, 12276−12286.

II. Simulation Methods

In the series of calculations reported here, a variety of molecular dynamics simulations and conformational energy minimizations were performed for α,α-trehalose by using the molecular mechanics program CHARMM.[36] The intramolecular energy of the solute was represented by a CHARMM-type force field designed for carbohydrates which has been used in a number of previously reported simulations of mono- and disaccharides.[37] In this all-atom potential function hydrogen bonds were modeled implicitly by appropriate choices for atomic partial charges and van der Waals parameters for hydrogen bond donor and acceptor atoms.[38] This approach is consistent with the way in which hydrogen bonding is represented in most empirical water force fields, including the TIP3P model used here.[39] The charge of the glycosidic oxygen atom was taken to be −0.4e, and the C1 and C5 charges were all adjusted to be 0.2e; the H1 and H5 charges retained the values of 0.1e used for aliphatic protons in the monosaccharides. As required by both the water model employed and the original assumptions made in the development of the solute energy parameters, the dielectric constant in all of the calculations reported here was 1.0. The carbohydrate force field contains no term to explicitly represent the anomeric or exo-anomeric effects, although such revisions have been previously suggested.[40] The importance of exo-anomeric effects for disaccharide conformations has long been debated,[41−43] and these should be most important in (1→1) disaccharides such as trehalose with overlapping anomeric effects.[22] The crystal structures[44,45] do indeed have torsion angles which place both C1 atoms gauche to the O5 atoms of the other ring, consistent with expectations from models of the exo-anomeric energy. In this context, however, it is interesting that in chiroptical studies of a synthetic analog of β,β-trehalose in which the glycosidic oxygen is replaced by a carbon atom, no evidence was found for any exo-anomeric effect.[46]

To assist in the interpretation of the calculated dynamics of the disaccharide, a relaxed, or adiabatic, Ramachandran-type conformational potential energy map[19] for trehalose *in vacuo* was prepared. The glycosidic torsion angles ϕ and ψ describing this two-dimensional space were defined as H1−C1−O1−C1′ and C1−O1−C1′−H1′. In this map, any strains in the internal geometry for each value of ϕ and ψ were relaxed by energy minimization to give the lowest energy for that point in the two-dimensional conformational space. All of the primary alcohol conformations of both rings, combined with the clockwise (designated "C") and counterclockwise, or reverse-clockwise (designated "R") hydrogen-bonded ring arrangements of the hydroxyl groups[47] were used as starting structures for energy minimizations for each (ϕ,ψ) point. These multiple starting geometires were used to overcome the multiple-minimum limitation inherent in energy minimizations[48] and to identify the lowest possible energy for each particular glycosidic conformation. Only $^4C_1$ conformations of the ring were considered, and no transitions to other ring conformations occurred during any of the minimizations. The energy surface was sampled on a 20° × 20° grid over the entire [−180°,180°] range of both ϕ and ψ and a contour map was prepared of the results.

Molecular dynamics simulations of α,α-trehalose in vacuum and in aqueous solution were also performed. Two 250-ps vacuum trajectories were calculated, one starting from the global minimum-energy conformation identified from the construction of the adiabatic energy map and one starting from the conformation seen in the dihydrate crystal structure. Two solution simulations were also carried out, again starting from the global minimum-energy geometry and from the X-ray crystal structure. The crystal structure of α,α-trehalose dihydrate[44,49] has one exocyclic primary alcohol group in the GT orientation, meaning *gauche* to O5 and *trans* to C4,[50] and one in the GG orientation (*gauche* with respect to both atoms), as seen in Figure 1b, breaking the pseudo-symmetry of the molecule (because of crystal contacts, the orientations of the various hydroxyl groups also differ between the two rings). The two crystallographically-resolved waters were not specifically included in the solution trajectory setup. The simulations were initiated by placing the trehalose molecule in the center of an equilibrated cubic box containing 512 TIP3P water molecules.[39,51] Those water molecules with oxygen atoms that overlapped with any of the solute heavy atoms were eliminated, leaving 488 solvent molecules for both simulations. The box length was then adjusted to 24.6433 Å, resulting in a density of 1.013 g/cm^3. The solvated system was subjected to simple cubic, minimum-image periodic boundary conditions, and long-range interactions were adjusted to smoothly approach zero by using a switching function[36] applied on a group-by-group basis between 10.0 and 12.0 Å.[52] The groups consist of entire water molecules or electrically neutral collections of adjacent atoms in the solute. Initial velocities for all atoms were selected at random from a Boltzmann distribution at 300 K. The equations of motion were then integrated as a microcanonical ensemble by using a Verlet integrator[53] with a step size of 1 fs. All chemical bonds to hydrogen atoms were kept fixed by using the SHAKE constraint algorithm.[54] The simulation starting in the crystal conformation had a 20-ps equilibration sequence followed by 130 ps of dynamics used for data collection and averaging. The solution simulation initiated in the vacuum global minimum-energy conformation had a 30-ps equilibration period, after which it was integrated for an additional 300 ps without further interference. During the equilibration periods the velocities were appropriately rescaled if the average temperature in a 2-ps interval deviated from 300 K by more than 3 K. Coordinate sets were saved every 10 fs for subsequent analysis. As a control, a 130-ps simulation of pure water was also conducted on a box of approximately the same size containing 512 water molecules at the same temperature and with similar startup protocols. During the production dynamics sequence, the total energy was well-conserved and the average temperature was stable at 300 ± 3 K.

In the crystal structure for trehalose both sugar rings are in the $^4C_1$ conformation,[55] and none of the MD trajectories exhibited any transitions to other ring conformations, since the rings are relatively rigid and are stabilized to transitions by high energy barriers. One consequence of this rigidity is that while the rings flex and breathe, and bonds stretch and bend, the various hydroxyl groups and aliphatic protons nonetheless remain on average at approximately fixed relative positions around the ring. As a result, the majority of the flexibility of the trehalose disaccharide comes from small torsional fluctuations about the glycosidic linkage bonds. Exploiting this rigidity, it is possible to identify the appropriate coordinate transformation that will map the instantaneous position and orientation of the ring onto its initial position. By using this coordinate transformation to remove the translational and rotational diffusion of the molecule, the position of every water molecule can be plotted relative to the functional groups on the ring, and an average solvent density at any point around the sugar can be calculated by averaging over the trajectory.[30,35,56] This approach is similar to the analysis of the anisotropic distribution of water molecules around amino acid groups constructed by Thanki et

(36) Brooks, B. R.; Bruccoleri, R. E.; Olafson, B. D.; Swaminathan, S.; Karplus, M. *J. Comput. Chem.* **1983**, *4*, 187−217.
(37) Ha, S. N.; Giammona, A.; Field, M.; Brady, J. W. *Carbohydr. Res.* **1988**, *180*, 207−221.
(38) Reiher, W. E. Ph.D. Thesis, Harvard University, 1985.
(39) Jorgensen, W. L.; Chandrasekhar, J.; Madura, J. D.; Impey, R. W.; Klein, M. L. *J. Chem. Phys.* **1983**, *79*, 926−935.
(40) Homans, S. W. *Biochemistry* **1990**, *29*, 9110−9118.
(41) Perez, S.; Marchessault, R. H. *Carbohydr. Res.* **1978**, *65*, 114−120.
(42) Thogersen, H.; Lemieux, R. U.; Bock, K.; Meyer, B. *Can. J. Chem.* **1982**, *60*, 44−57.
(43) Wiberg, K. B.; Murcko, M. A. *J. Am. Chem. Soc.* **1989**, *111*, 4821−4828.
(44) Brown, G. M.; Rohrer, D. C.; Berking, B.; Beevers, C. A.; Gould, R. O.; Simpson, R. *Acta Crystallogr.* **1972**, *B28*, 3145−3158.
(45) Jeffrey, G. A.; Nanni, R. *Carbohydr. Res.* **1985**, *137*, 21−30.
(46) Duda, C. A.; Stevens, E. S. *J. Am. Chem. Soc.* **1993**, *115*, 8487−8488.
(47) Ha, S. N.; Madsen, L. J.; Brady, J. W. *Biopolymers* **1988**, *27*, 1927−1952.
(48) Scheraga, H. A. *Biopolymers* **1983**, *22*, 1−14.
(49) Taga, T.; Senma, M.; Osaki, K. *Acta Crystallogr.* **1972**, *B28*, 3258−3263.
(50) Marchessault, R. H.; Perez, S. *Biopolymers* **1979**, *18*, 2369−2374.
(51) Durell, S. R.; Brooks, B. R.; Ben-Naim, A. *J. Phys. Chem.* **1994**, *98*, 2198−2202.
(52) Tasaki, K.; McDonald, S.; Brady, J. W. *J. Comput. Chem.* **1993**, *14*, 278−284.
(53) Verlet, L. *Phys. Rev.* **1967**, *159*, 98−103.
(54) van Gunsteren, W. F.; Berendsen, H. J. C. *Mol. Phys.* **1977**, *34*, 1311−1327.
(55) Stoddart, J. F. *Stereochemistry of Carbohydrates*; Wiley-Interscience: New York, 1971.
(56) Brady, J. W. *Forefronts/Cornell Theory Center* **1993**, *9*, 7.

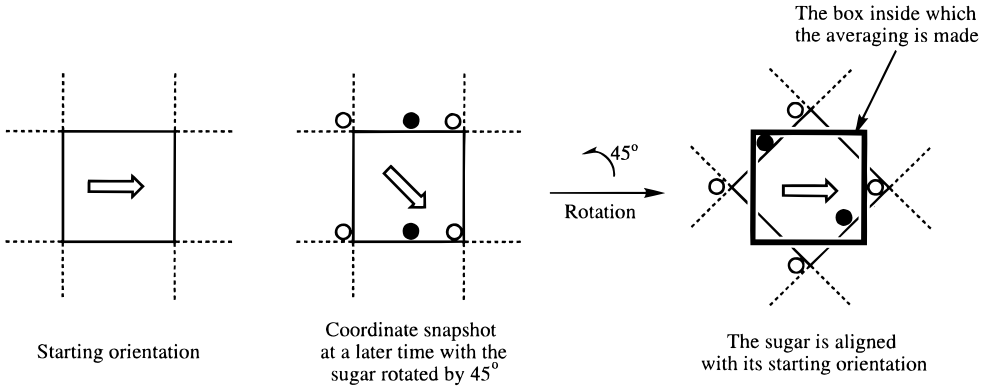

Figure 2. A schematic illustration of the effects of the rotational coordinate transformation on the density averaging. The sugar is represented by an arrow in this drawing and specific water molecules and their periodic images by open and filled circles. The box inside which the averaging is made, which is not periodic and does not rotate, is indicated by heavy lines.

al. by averaging over protein structures reported in the crystallographic data base.[57] Similar methods have been used to extract the anisotropic structure of pure liquids from simulations[58−60] and to place water molecules in protein crystal structures.[61,62]

We have used such an approach in the present simulations to calculate the full three-dimensional, anisotropic distribution of solvent water molecules around the trehalose solute. For every saved coordinate frame of the trajectory the CHARMM program was used to calculate the best least-squares overlap of the instantaneous positions of the reference atoms with their initial positions, and this transformation was applied to every atom of the system, including the water atoms. The primary box was then partitioned into small cubes 0.342 Å on a side, and the density of solvent oxygen atoms in each cube was averaged over the trajectory. The averaging could be accomplished by a direct count average, but because we intend to apply this procedure to the calculation of electron densities in crystals for comparison with diffraction experiments, we chose to assign a normalized Gaussian distribution function to each water oxygen atom and to average the values of these density functions. This Gaussian function could be scaled to approximate the expected electron distribution around such an atom, providing an estimate of the electron density in each cubic box. In such a case, of course, it would also be necessary to place similar distributions around each of the sugar atoms and the water protons. In the present application, where we are interested in the number density of water oxygen atoms in each box, this procedure will lead to some smearing out of the solvent densities, since the Gaussian distribution function will result in some density for a particular water oxygen being counted in the boxes adjacent to the one in which it actually is located. This is not entirely undesirable, since it will have the effect of smoothing out the inevitable fluctuations due to noise in the populations of each box. In the present analysis, a narrow Gaussian function was used with the half-maximum falling at the van der Waals radius of the oxygen atom. No functions were placed on any of the atoms other than the water oxygens.

The solvent densities averaged over the simulation can be contoured in three dimensions in the same way that electron density maps are contoured in crystal diffraction studies. In the present analysis we have used the CHAIN program[63] to accomplish and display this contouring. The average bulk water oxygen density was evaluated from the simulations, and the solvent densities, which can be either greater than or less than the average bulk density, were contoured in terms of the percentage deviation above or below the average bulk value. The CHAIN program uses a line-mesh to represent the surface that encloses all regions with density values above or below the desired value, using a spline function to fit a continuous, smooth contour to the surface. Various two-dimensional cross sections of this three-dimensional density were also calculated.

As indicated above, the simulations were performed in a cubic box with periodic boundary conditions. The corners of the box are further away from the solute than the centers of the sides of the box, and could in principle be discarded through the application of truncated octahedral boundary conditions to save computation time.[64−66] However, their presence improves the physical approximation since they represent part of a "solvation shell" for the trehalose that is at a greater distance from the solute than the majority of the waters in the box, and thus help constitute a region of more bulk-like water less influenced by the sugar. Unfortunately, in the calculation of the average solvent densities around the solute, it is not possible to construct useful average densities for these corners of the original box. Figure 2 illustrates the reason for this problem. Consider the case of a trajectory "snapshot" at some arbitrary time **t** at which the molecule has rotated 45° with respect to its original orientation (effects of translation are removed through the appropriate translation of the center of mass to its starting position). In rotating the frame onto the original orientation, the solvent molecule indicated by the black circle would appear in the averaging in the original cubic box twice, once in its actual location near the head of the schematic arrow, and once, as its image (from the application of the periodic boundary conditions), in the corner. However, the water molecule represented by the open circle and its images, in the corner of the unrotated box at time **t**, would not appear in the averaging at all, and thus its contribution to the average solvent density in the primary box would be lost. The net effect of this procedure is that the resulting population densities are not a periodic function, and the values are only reliable inside a sphere with its origin at the center of the box and with a radius of one half the box length.

For a monosaccharide, this averaging procedure has been found to work quite well in delimiting the regions of solvent concentration,[30] but an additional problem arises when the molecule is more flexible, since location of the reference frame on one of the rings of the disaccharide, for example, has the effect of making all of the flexibility about the glycosidic linkage appear as a larger oscillation of the second ring relative to the first, thus greatly smearing out the distributions relative to the second ring, and losing much to the structuring detail. For this reason, these methods would not be applicable to a very flexible molecule, or even to a long polymer that had fairly rigid individual linkages, but where the large number of monomers resulted in a large cumulative motion of one end of the chain relative to the other. In the present case, the torsional fluctuations about the glycosidic linkage were comparatively small for the most stable conformation, so the reference coordinate frame could also be placed on the three atoms of the linkage (C1−O1−C1′). This compromise works well for trehalose, losing some

(57) Thanki, N.; Thornton, J. M.; Goodfellow, J. M. *J. Mol. Biol.* **1988**, *202*, 637−657.
(58) Svishchev, I. M.; Kusalik, P. G. *J. Chem. Phys.* **1993**, *99*, 3049−3058.
(59) Svishchev, I. M.; Kusalik, P. G. *J. Chem. Phys.* **1994**, *100*, 5165−5171.
(60) Kusalik, P. G.; Svishchev, I. M. *Science* **1994**, *265*, 1219−1221.
(61) Lounnas, V.; Pettitt, B. M.; Phillips, G. N. *Biophys. J.* **1994**, *66*, 601−614.
(62) Lounnas, V.; Pettitt, B. M. *Proteins* **1994**, *18*, 133−147.
(63) Sack, J. S. *J. Mol. Graphics* **1988**, *1988*, 224−225.
(64) Adams, D. J. *Chem. Phys. Lett.* **1979**, *62*, 329−332.
(65) Remerie, K.; Engberts, J. B. F. N.; van Gunsteren, W. F. *Chem. Phys.* **1986**, *101*, 27−44.
(66) Allen, M. P.; Tildesley, D. J. *Computer Simulation of Liquids*; Clarendon Press: Oxford, 1987.

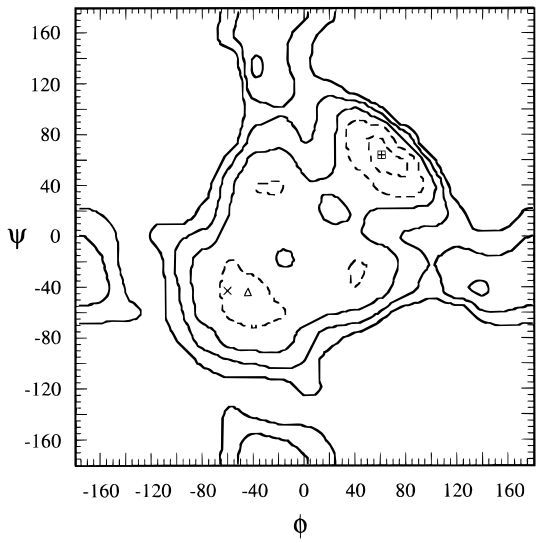

Figure 3. The calculated vacuum adiabatic conformational energy map for α,α-trehalose. Contours are indicated in 2-kcal/mol intervals above the global minimum, indicated by a crossed box. The contours at 2 and 4 kcal/mol are drawn with dashed lines to better distinguish the off-diagonal minima from the two low maxima on the diagonal line. The crystal structure is indicated by the symbol "×", and the local minimum nearest to the crystal structure is indicated by a triangle.

Table 1. The Locations and Energies (in kcal/mol, relative to the global minimum) of the Minima Identified in the Adiabatic Mapping of α,α-Trehalose

minimum	ϕ (deg)	ψ (deg)	energy (kcal/mol)
1	61	64	0.00
2	−44	−44	3.36
3	41	−33	3.65
4	−33	41	3.65
5	−40	140	5.60
6	140	−40	5.60

detail for each ring, but allowing a general mapping of the solvent density around both rings simultaneously (see below).

III. Results and Discussion

Figure 3 presents the calculated vacuum adiabatic conformational energy map for α,α-trehalose. The diagonal symmetry of the map is a consequence of the structural symmetry of the molecule. The surface has six principal minima (Table 1), two located on the diagonal line of symmetry and four occurring as two symmetrically-located, off-diagonal pairs. The global minimum is located at (61°,64°). This conformation is stabilized by an intramolecular hydrogen bond between the O2 hydroxyl groups of the two rings (see Figure 4). The position of the minimum lies slightly off the diagonal line of symmetry on the map, perhaps because the presence of the hydrogen bond, which has a donor−acceptor directionality, introduces a small asymmetry into the structure; however, a symmetrically located companion minimum lies at (64°,61°) due to the overall pseudosymmetry of the molecule. A broad secondary minimum 3.36 kcal/mol higher in energy than the global minimum-energy conformation is centered around (−44°,−44°). This local minimum-energy well contains the experimentally-determined crystal structure,[44] indicated by an "×" in Figure 3 and located approximately at (−60°,−43°), as well as the conformations estimated from NMR and chiroptical experiments.[12−14,17] Two symmetrically-placed, off-diagonal local minima were found at (−33°,41°) and (41°,−33°), approximately 3.65 kcal/mol above the global minimum, but only 0.29 kcal/mol above the experimental local minimum at (−44°,−44°). These conformations are each stabilized by one intramolecular hydrogen bond, either between O2 and O6′ or between O2′ and O6. Two small peaks are also located on the diagonal line, around (22°,22°) and (−18°,−18°).

This map shares a number of qualitative features with the MM3 map previously prepared by Dowd et al.,[22] but also differs in several important respects. One of these differences is that while generally relatively rigid, the trehalose molecule in the present study was found to be considerably more flexible in vacuum than with the MM3 force field. The global minima on the two surfaces are different as well. The global minimum on the present map is not a low-energy conformation on the MM3 surface. Part of the reason is that the former map was calculated by using a dielectric constant of 4.0, which would have the effect of screening electrostatic interactions so strongly as to almost eliminate hydrogen bonding. Since the global minimum on the present map is stabilized by an intramolecular hydrogen bond, the dielectric screening in the MM3 calculation would contribute to making this conformation less favored. In addition, in the present mapping, the severe crowding in the global minimum-energy structure significantly distorts the C1−O1−C1′ bond angle to 119°, which would be more energetically costly with the "stiffer" MM3 parameters. The subsidiary off-diagonal minima in the present map at (−33°,41°) and (41°,−33°) correspond to the MM3 minima at (−29°,25°) and (25°,−29°), but on the MM3 map these positions are 4.7 kcal/mol higher in energy than the conformer at (−45°,−45°), while on the present map these subsidiary minima are only 0.29 kcal/mol above the experimental minimum, since they are also stabilized by hydrogen bonds. The local minimum on the present map at (−44°,−44°) corresponds well with the global minimum on the MM3 surface at (−45°,−45°).

The lowest-energy structure in the global minimum well had the TGTG,RC conformation,[47] while the lowest-energy structure in the experimental well has the TGTG,CC conformation. The crystal structure has the GTGG conformation for the primary alcohols; because of hydroxyl group hydrogen bonds to the two included water molecules, the C−R scheme does not strictly describe the crystal structure, although the ring with the primary alcohol in the GG conformation is approximately reverse, or counterclockwise (R). No TG conformations for the exocyclic primary alcohol groups were considered in the MM3 study, but probably would not have had a low energy with that force field since this conformation is stabilized in the present study by an internal hydrogen bond between O4 and O6 of the same ring. The TG conformation for primary alcohols is rarely seen experimentally in glucosic carbohydrates, and appears in simulations with the present force field because Coulombic repulsions between the O6 and O5 atoms destabilize the gauche conformations more than is appropriate from quantum mechanics,[67] allowing the internal hydrogen bond of the TG conformation to dominate the rotameric equilibrium.

Although disaccharide conformations are often interpreted in terms of vacuum energy surfaces of the type presented here, in real systems carbohydrates are typically found in an aqueous environment, and solvent water is expected to have significant effects on the conformational structure. The force field used here was designed for condensed-phase simulations, in which the environment is included explicitly, and it has previously been observed that simulations without this solvent can lead to artificial behavior.[47,68] Since dimer conformations are actually determined by the system free energy rather than the simple

(67) Murcko, M. A.; DiPaola, R. A. *J. Am. Chem. Soc.* **1992**, *114*, 10010−10018.
(68) Ueda, K.; Brady, J. W. *Biopolymers* **1996**, *38*, 461−469.

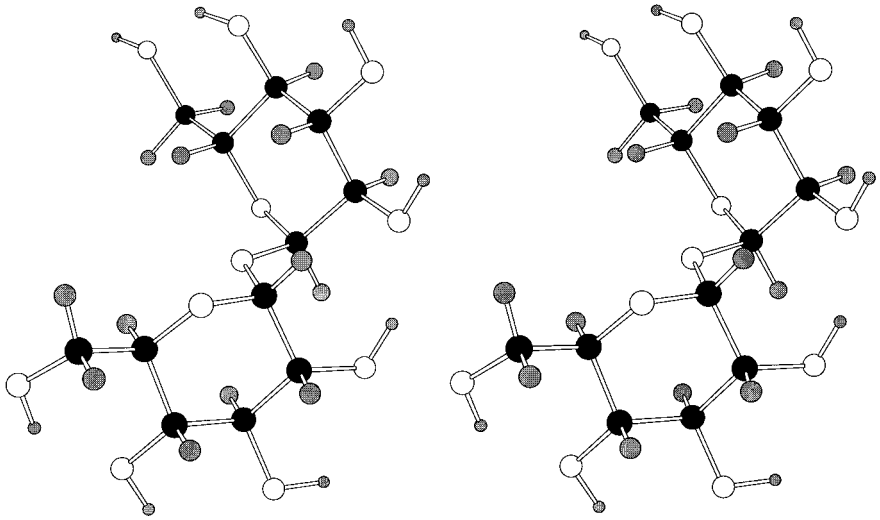

Figure 4. The global minimum energy conformation identified from the adiabatic energy map of Figure 2.

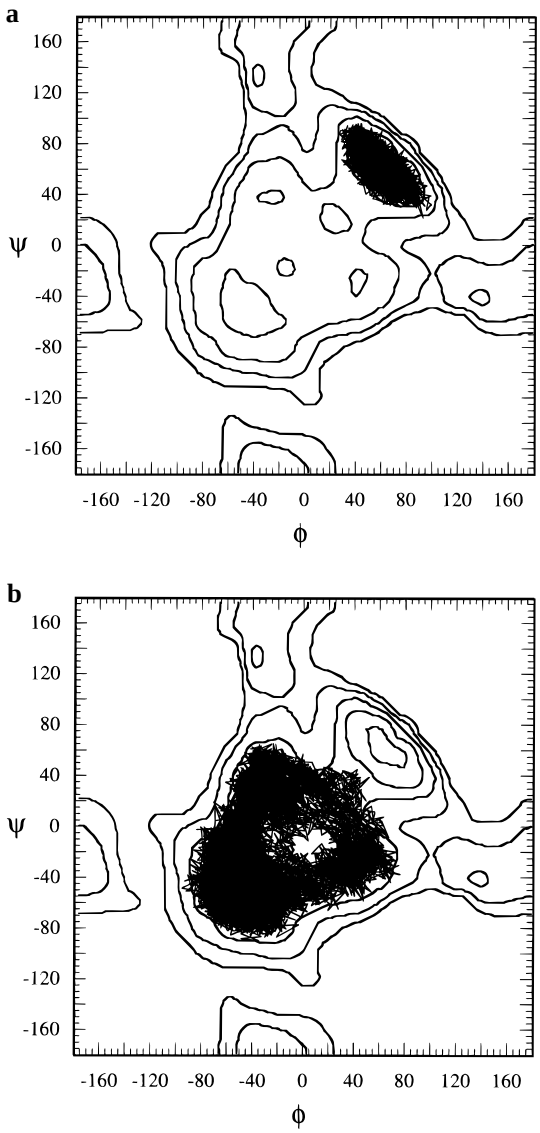

Figure 5. Superposition of vacuum molecular dynamics trajectories in (ϕ,ψ)-space upon the vacuum adiabatic energy map: (a) trajectory starting from the global minimum-energy structure; (b) trajectory starting from the crystal structure.

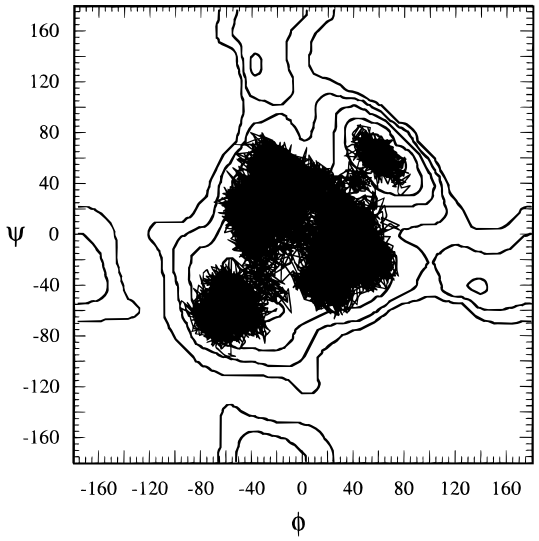

Figure 6. Superposition of the solution trajectory that started from the vacuum global minimum-energy geometry onto the vacuum adiabatic energy map.

mechanical potential energy, a map of the conformational potential of mean force, including the average contribution of the solvent, would be more appropriate. Trehalose appears to be an example of a disaccharide whose conformation is strongly affected by hydration. Vacuum MD simulations at 300 K initiated from the global minimum energy structure and the crystal structure tended to remain contained within the 4-kcal/mol contour (>6 kT) above the local energy well in which they began (Figure 5). However, in the vacuum global minimum-energy geometry identified from the present relaxed mapping, there is a direct hydrogen bond between the O2 and O2′ hydroxyl groups, which apparently causes this conformation to have the lowest potential energy. In aqueous solution, it should be possible for this internal hydrogen bond to exchange for hydrogen bonds to solvent water molecules. Such an exchange of an intramolecular hydrogen bond for alternate hydrogen bonds to solvent has been observed in previous simulations of sucrose[69] and neocarrabiose,[68] and was also found to occur in the present simulations of trehalose. As can be seen from Figures 6 and 7, the solution trajectory which started from the global minimum-energy geometry quickly began to shift toward the experimental geometry, first dividing its time between the two symmetrically related conformers around (−33°,41°) and (41°,−33°), before making a final transition to the well containing the crystal

(69) Engelsen, S. B.; Herve du Penhoat, C.; Perez, S. *J. Phys. Chem.* **1995**, *99*, 13334−13351.

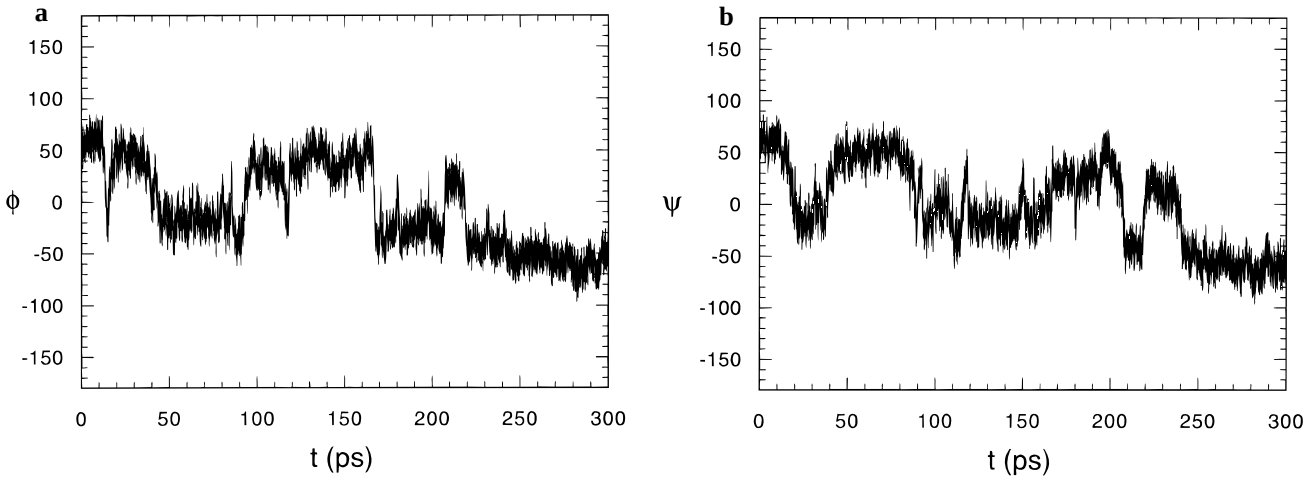

Figure 7. Individual histories of the torsional angles ϕ and ψ for the solution trajectory that began in the vacuum global minimum energy conformation but ended in the experimental conformation.

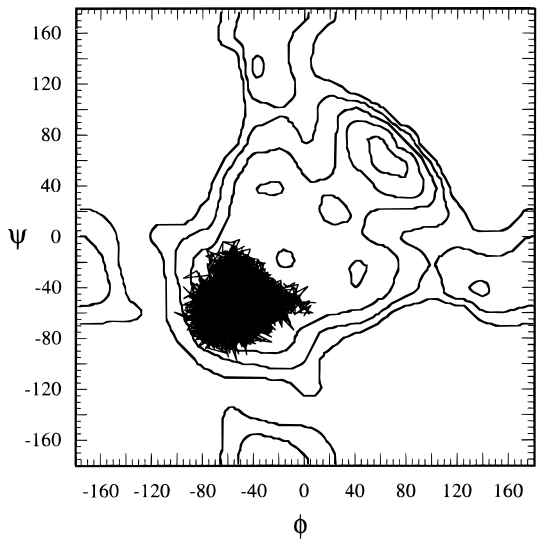

Figure 8. Superposition of the solution trajectory that started from the crystal structure onto the vacuum adiabatic energy map.

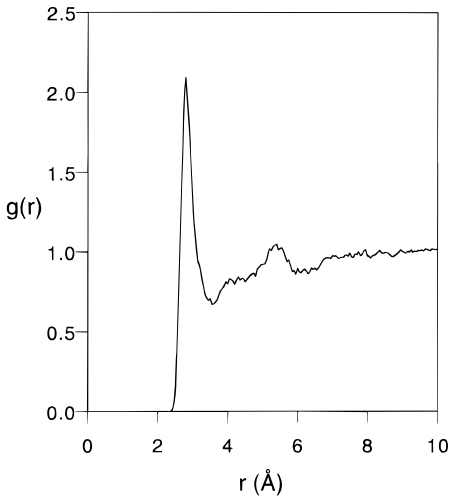

Figure 9. The pair distribution function for water oxygen atoms around one of the O3 atoms of trehalose as calculated from the MD simulation in the experimental conformation. This distribution is typical of those for the other hydroxyl groups.

conformation around 240 ps. This final conformation appears to be indefinitely stable.

The separate trajectory that started in this secondary, experimental well remained in this conformation throughout the simulation (Figure 8), which in conjunction with the first trajectory that made a spontaneous transition to this geometry, suggests that this structure is the global minimum free energy conformation in solution. Various average properties for trehalose in solution were computed from this 130-ps simulation. From the simulation, the average values of the linkage angles were (−54°,−54°), close to the local minimum-energy structure and in reasonable agreement with the NMR and chiroptical estimates.[14,17] However, the presence of the solvent seems to have induced a slight shift in the conformation of about 10° to larger angles. The root-mean-square fluctuations in these angles during the simulation were 13.6° and 12.9°, about the same as found in the simulation by Donnamaria et al.,[31] indicating a relatively rigid equilibrium structure. These fluctuations were roughly comparable to, but slightly larger than, those seen for maltose in solution.[28] It is interesting that no special exoanomeric energy terms were needed to reproduce the experimental conformational behavior, as was also found in previous simulations with this force field.[68] During the course of this simulation, the two primary alcohol groups underwent a number of transitions. Both groups sampled all three conformations, although the exocyclic groups spent the majority of their time in the GT conformation. The hydroxyl groups made frequent rotational transitions during the simulation.

These hydroxyl groups of the sugar molecule were extensively hydrogen bonded to solvent in the stable equilibrium conformation. Figure 9 presents an example of a hydroxyl oxygen−water oxygen pair correlation function. This distribution exhibits a sharp, narrow first peak at 2.8 Å, with a prominent first minimum at 3.4 Å, as is typical for hydrogen bonds to water.[25,27,70] For counting purposes solute−solvent hydrogen bonds were defined as interactions having oxygen−oxygen distances less than 3.4 Å and donor−proton−acceptor angles of 120° or greater.[28] The average number of such hydrogen bonds made by each hydroxyl group is listed in Table 2. The total number of hydrogen bonds to solvent made by the trehalose solute, averaged over the simulation, was 22.5, which does not differ substantially from the 22.7 observed for maltose.[28] However, previous MD simulations of sugars have demonstrated that even such a small difference as this can result in a large difference in solute−solvent interaction energy.[35] This number is somewhat reduced from the approximately 24 solvent hydrogen bonds that in principle could be possible for the eight

(70) Rossky, P. J.; Karplus, M. *J. Am. Chem. Soc.* **1979**, *101*, 1913−1937.

Table 2. Trajectory-Averaged Number of Hydrogen Bonds to Solvent Made by Each Oxygen Atom of the Sugar

atom	residue 1	residue 2
O1	0.57	
O2	2.68	2.79
O3	2.58	2.50
O4	2.23	2.37
O5	0.74	0.78
O6	2.53	2.74
total	11.33	11.18

Table 3. Hydroxyl Groups on Different Rings Found To Be Bridged by Hydrogen Bonds to a Common Water Molecule, and the Frequency with Which Each Was Observed during the Simulation[a]

hydroxyl pair	% of trajctory time during which water bridging was obsd
O2−O2′	6.7
O2−O4′	21.4
O2−O6′	2.3
O4−O2′	11.5
O5−O5′	9.3
O6−O2′	9.9
O6−O5′	2.9

[a] Transient bridges observed in less than 1% of the trajectory time are omitted. For the purposes of this enumeration, a hydrogen bond was defined as both O−O distances being less than 3.5 Å and both donor−proton−acceptor distances being greater than 120°.

hydroxyl groups of trehalose (30 counting the two ring oxygens and the glycosidic oxygen atom), since each hydroxyl could form up to three such hydrogen bonds, one as a donor and two as an acceptor (to its two lone pairs). As can be seen from the table, none of the hydroxyl groups actually makes this ideal number of bonds, much as was seen for other sugars,[28,35] and each of the ether oxygen atoms makes less than one bond on average. However, this total number of hydrogen bonds to solvent is nearly twice that reported by Donnamaria et al.,[31] who estimated that their observed slight decrease in water−water hydrogen bonds could be explained if the disaccharide made 10 hydrogen bonds to the solvent. In that simulation, the majority of the energy parameters used were taken from the GROMOS force field, but the atomic partial charges were taken without scaling from a separate AM1 calculation, a procedure known to give values too small to be used in explicit solvent calculations.[71] The lower charges used for the sugar hydroxyl oxygen and hydrogen atoms substantially reduced the hydrogen-bonding character of these groups, as can be seen from their reported pair distribution functions. In that earlier study these functions have their broad first peaks centered around 3.5 Å, with a much lower peak height, and have their first minima around 4.5−5.0 Å, thus more closely resembling hydrophobic hydration[72−74] than hydrogen bonding with its characteristic sharp first peak,[27,75] as in Figure 9. In the present simulation, as in the maltose case, nearly one third (32.2%) of the hydrogen bonds made to the solvent by the sugar were of the type in which the water molecule made two hydrogen bonds to the solute, to two adjacent hydroxyl groups. Many of these second hydrogen bonds had significantly distorted bond angles due to the constraints imposed by the relative positions of the hydroxyl groups in the structure of the sugar molecule.

Unlike the maltose case, a number of hydrogen bonds were observed for water molecules bridging between hydroxyl groups on different rings. Some of these water bridges were very much like those observed in the crystal structure of the dihydrate, where there are two water molecules hydrogen bonded to hydroxyl groups on different rings of the disaccharide, bridging between the O4 and O2′ and O2′ and O6 hydroxyl pairs[44,49] (see Figure 1b). In the MD simulation both of these crystallographic positions were occupied by water molecules during the majority of the trajectory, which were often engaged in such simultaneous bridging hydrogen bonds. It would appear that these hydrogen bonds stabilize the experimental conformation in solution relative to the global vacuum minimum energy conformation, since they replace the intramolecular hydrogen bond between the two O2 hydroxyl groups in that structure (see above). A very similar situation has been observed in an MD simulation of neocarrabiose in aqueous solution, where an intramolecular hydrogen bond in vacuum is replaced in solution by a bridging water molecule that produces a shift to the experimentally observed conformation.[68] In the trehalose simulation, bridging hydrogen bonds are present 48% of the trajectory time, with a water bridging between the O4 group on one ring and the O2 group of the other being the most common type. Bridges between O2 and O2′, O5 and O5′ (with the water serving as a double donor), and O2′ and O6, as in the crystal, also occurred frequently. During the simulation, the distances between the two O2−O6 atom pairs from opposite rings were 6.3 and 5.7 Å, with root-mean-square fluctuations of only 0.7 and 0.8 Å. These distances, while permitting bridging interactions by hydrogen-bonded water molecules, are too great to allow direct hydrogen bonding between these two groups as was observed in the simulations by Donnamaria et al.[31]

It has been suggested that water molecules bridging between two groups capable of hydrogen bonding, such as hydroxyls, can contribute a considerable free energy of stabilization to relative positions of the two groups which do not allow direct hydrogen bonding between them. Ben-Naim has estimated that this stabilization energy can be as important in determining biopolymer conformations as hydrophobic association,[51,76−78] although Sun and Kollman have recently argued that the magnitude of this effect is much smaller.[79] It is possible that such hydrophilic interactions are stabilizing the experimental conformation in the present simulations, but it is not possible from these calculations to make a quantitative estimate of the magnitude of any such contribution. However, in the present case, it seems likely that the experimental geometry would be the favored solution structure even without any such contribution. The solution conformation is a local minimum on the vacuum surface, and only the presence of the intramolecular hydrogen bond makes the (+61°,+64°) conformation the global minimum. In the presence of the solvent, there is no energy penalty to breaking this internal hydrogen bond, and the inherent preference for the experimental conformation would then dominate the equilibrium without any additional stabilization needed. This possibility would be consistent with the observation that 52% of the trajectory time these water molecule bridges are not present.

The hydration requirements of the complex disaccharide, along with the shared hydrogen bonding, imposed significant anisotropic structuring on the solvent adjacent to the sugar, with water molecules preferentially occupying specific sites relative

(71) Gao, J. *J. Phys. Chem.* **1992**, *96*, 6432−6439.
(72) Broadbent, R. D.; Neilson, G. W. *J. Chem. Phys.* **1994**, *100*, 7543−7547.
(73) Swaminathan, S.; Harrison, S. W.; Beveridge, D. L. *J. Am. Chem. Soc.* **1978**, *100*, 5705−5712.
(74) Geiger, A.; Rahman, A.; Stillinger, F. H. *J. Chem. Phys.* **1979**, *70*, 263−276.
(75) Ferrario, M.; Haughney, M.; McDonald, I. R.; Klein, M. L. *J. Chem. Phys.* **1990**, *93*, 5156−5166.
(76) Ben-Naim, A. *J. Chem. Phys.* **1989**, *90*, 7412−7425.
(77) Mezei, M.; Ben-Naim, A. *J. Chem. Phys.* **1990**, *92*, 1359−1361.
(78) Ben-Naim, A. *J. Chem. Phys.* **1990**, *93*, 8196−8210.
(79) Sun, Y.; Kollman, P. *J. Phys. Chem.* **1996**, *100*, 6760−6763.

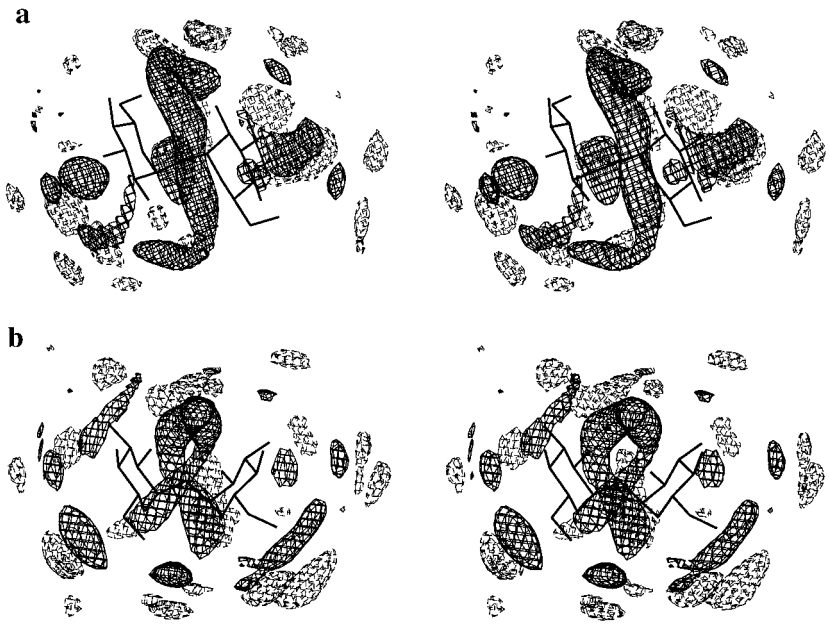

Figure 10. Contours of solvent density around the α,α-trehalose molecule as calculated from the MD simulation by using a reference frame fixed on the glycosidic linkage. The solid contour grid encloses those regions with a density 50% greater than the bulk density, and the dashed contour grid encloses negative deviations 20% less than the bulk density. Two different orientations are illustrated for clarity, rotated by approximately 90°.

Figure 11. The contours of positive density deviations displayed in Figure 10, with 130 instantaneous solute conformations spaced at 1-ps intervals, oriented such that their C1−O1−C1′ atoms overlapped as much as possible, illustrating the range of the relative motions in the rings caused by the glycosidic angle fluctuations. This view has been rotated by approximately 180° from that of Figure 10a.

to the carbohydrate functional groups. Figure 10 displays the anisotropic solvent density averaged over the 130-ps simulation in the experimental conformational energy well, calculated by mapping the instantaneous conformation onto the initial C1−O1−C1′ positions (see Methods). The long tube-shaped cloud of density wrapped around the center of the molecule contains all those water positions which can make bridging hydrogen bonds between hydroxyl groups on different rings. In particular, both of the positions occupied by the crystallographic water molecules in the dihydrate crystal[44] (Figure 1b) fall within this long, tube-shaped cloud, indicating that these solvent sites are favored in solution as well. The open end of this U-shaped tube is occupied by a small discrete cloud that corresponds to the water molecules hydrogen bonded to the O5 atoms. In general, it can be seen from this figure that the structuring imposed on the water by trehalose is quite complex.

Although the conformational fluctuations of the trehalose are relatively small, the apparent degree of solvent structuring exhibited in Figure 10 is actually substantially reduced by these fluctuations since their effect is to "smear out" the density as the rings move relative to the three atoms of the glycosidic linkage. This is why the densities seen in Figure 10 are smallest at the far ends of the rings, where the arc swept out by these small fluctuations is the greatest. Figure 11 superimposes 130 instantaneous conformations of the disaccharide selected at 1-ps intervals, all rotated such that their C1−O1−C1′ atoms overlap as closely as possible to illustrate this flexibility. As can be seen, the area swept out even by these relatively small fluctuations is extensive enough to obscure the solvent structuring around the far edges of the rings in this reference frame. Figure 12 displays a contouring of the solvent densities calculated from the same trajectory, but using a reference frame fixed with respect to one of the rings, so that this ring is rotated onto its original position for every frame of the simulation. Applying this transformation to all of the coordinates has the effect of making all of the relative motion of the two rings appear as motion of the second ring, thus increasing the extent to which its structured solvent density is smeared out, but providing a much clearer picture of the detailed structuring imposed by the first ring. As in the previous case, 130 individual sugar structures are overlain in this figure to illustrate the range of the conformational fluctuations. In this special case, the artifactual focus on the structure around just one of the rings is less important because of the symmetry of the molecule and its structured solvent. The calculated distributions are very similar regardless of which ring is used for the reference frame.

By using a ring-centered reference frame, it can be seen that the nature of the structuring around the individual rings is very similar to that observed in our previous simulations of monosaccharides.[30,35,80] In particular, water molecules tend to be localized between adjacent hydroxyl groups where they can

(80) Liu, Q.; Brady, J. W. *J. Phys. Chem.* **1997**, *B101*, 1317−1321.

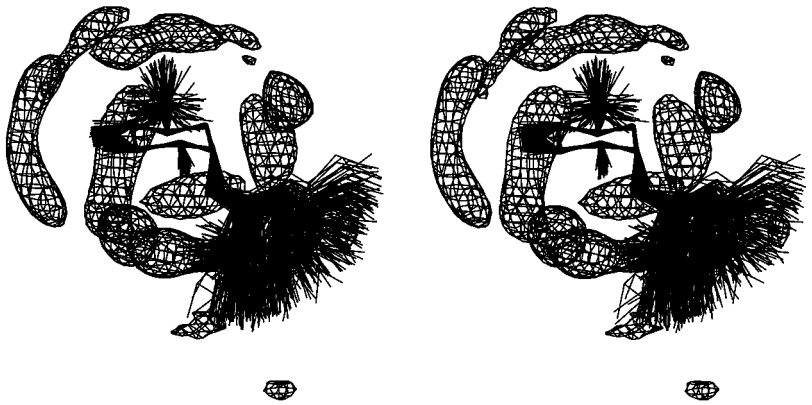

Figure 12. Contours of positive solvent density around the α,α-trehalose molecule as calculated from the MD simulation by using a reference frame fixed on one of the sugar rings. As in Figure 11, 130 instantaneous conformations of the carbohydrate from the trajectory are displayed to illustrate the wide region traversed by the second ring, relative to the first, causing the solvent density to be smeared out.

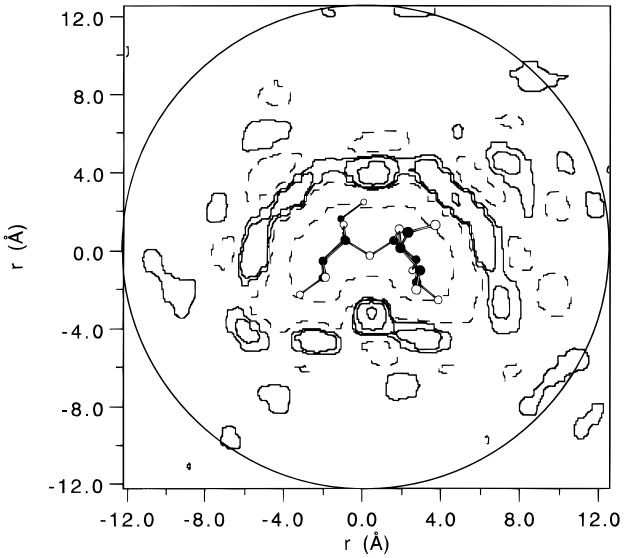

Figure 13. Two-dimensional cross section of the solvent density in a plane through the C1, O1, and C1′ atoms. Density contours are at 10, 20, 50, and 90% above bulk density (solid contours) and 10 and 90% below bulk density (dashed contours). In this figure, the circle indicates the region in which the densities are statistically meaningful; sampling in the region outside this radius is affected by the transformation problems discussed above.

simultaneously make hydrogen bonds to both solute groups. Other clouds of density above and below the rings correspond to the water molecules hydrating the hydrophobic surfaces consisting of aliphatic protons. The tube of density wrapped around the center of the molecule in Figure 10 breaks up in to more localized positions in this reference frame, generally centered in positions to make optimum hydrogen bonds to the hydroxyl on the reference ring. Figure 13 displays a two-dimensional cross section of the solvent density in a plane through the C1−O1−C1′ atoms. The well-defined second-shell peaks, in one case quite intense, make clear the extensive structuring imposed on the solvent. The highest intensity region of Figure 13 is "below" and between the two rings where the plane intersects the long density tube that runs around the center of the molecule.

The extensive range of the structuring imposed on water by sugars such as trehalose is further revealed by comparison to the amount of inherent structure found in pure water. Liquid water retains a considerable degree of the local tetrahedral structure characteristic of the solid phase, although this structuring does not extend far out into the bulk liquid around any particular molecule as it would in the regular lattice of ice. Soper has described a procedure for estimating this structuring in liquid water by constructing the intermolecular orientational correlation function from measured partial structure factors using a spherical harmonic expansion,[5] and Kusalik and Svishchev[60] have calculated the structuring from MD simulations using three empirical models of water, including the SPC/E[34] and TIP4P[39] energy functions. Although some differences were found between the different water models, all exhibited similar qualitative features and were in good agreement with the experimental estimate. Figure 14 displays the three-dimensional contouring of this density for one of the water molecules from the present control simulation of pure TIP3P water. Far better statistical convergence for this density could be obtained by averaging together this structuring around each of the equivalent water molecules in this simulation, but by considering the density around only one molecule treated as a single, separate solute, the statistical fluctuations in the distribution will be of the same order as those in the sugar solution, thus facilitating comparison. As can be seen, the distribution of nearest-neighbors is quasitetrahedral, and qualitatively similar to those reported previously for the other water models. As was found in the previous studies, the ellipsoidal clouds adjacent to the two protons are more intense and spatially localized than the broader band of density in the direction of the lone pairs[5,60] (which, of course, are not explicitly present in TIP3P water). The density band for donor neighbors has higher densities in the tetrahedral directions as the result of packing constraints; this character is emphasized by Figure 14b, where the density is contoured at a higher level. However, when contoured at a lower level, as in Figure 14a, these two clouds merge into a continuous donor density band, with positions directly in between the tetrahedral directions being possible. This geometry would correspond to only one donor neighbor, and an overall coordination number of three, as suggested by Soper.[5] Of more importance for the present discussion, however, is the complete absence of significant structuring beyond the first solvation shell. From the two-dimensional cross section of the anisotropic density around this water molecule, shown in Figure 15, it can be seen that there is virtually no statistically significant structure beyond the first shell (the asymmetry of the very few other small peaks indicates that they are noise). This feature is in sharp contrast to the case for the trehalose solution with the same water model (Figure 13), as well as for the various pentose sugars previously studied,[30,35] where a distinct second shell is seen, with significant structuring even at much greater distances. From this comparison, it is apparent that the sugars impose very extensive, long-range collective structure on the solvent molecules. There does not appear to be any evidence that this

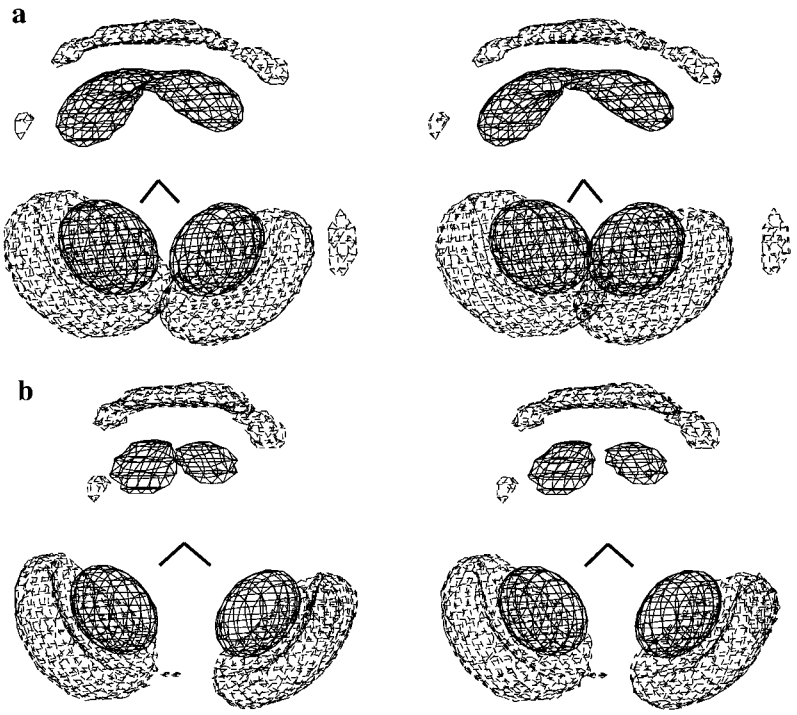

Figure 14. Contours of solvent density around a single water molecule in a control simulation of pure water. (a) The solid contour grid encloses those regions with a density 27% greater than the bulk density. (b) The same data as in part a, but with the solid contour enclosing regions with a density 35% greater than bulk. In both parts the dashed contour encloses regions of density 10% below the bulk value.

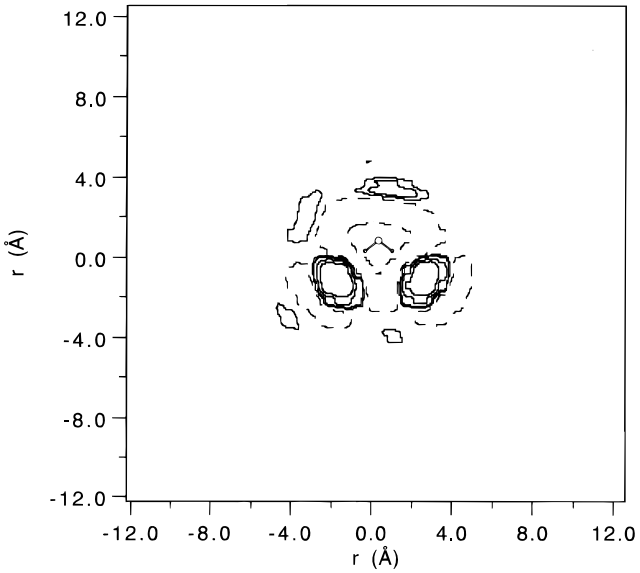

Figure 15. Two-dimensional cross section of the water density around a single water molecule in a control simulation of pure water. Density contours are at 10, 20, 50, and 90% above bulk density (solid contours) and 10 and 90% below bulk density (dashed contours).

structure is that of some underlying liquid lattice, as was suggested in early models of sugar hydration.[81,82]

The water self-diffusion coefficient was estimated for both the solution and pure water simulations from the slope of the mean-square displacement as a function of τ, evaluated in the diffusive limit by taking the tangent at 65 ps. In the solution simulation, the self-diffusion coefficient for all of the water molecules averaged together, 4.2×10^{-5} cm^2 s^{-1}, was 20% lower than that for pure TIP3P water, 5.2×10^{-5} cm^2 s^{-1}, in a box of the same size in the control simulation. This value for pure TIP3P water is approximately twice the experimental number, probably because of the less extensive structuring in liquid water with this model, and is somewhat larger than that found in a previous study of this water model,[52] 4.6×10^{-5} cm^2 s^{-1}, apparently due to the shorter simulation time available in our earlier simulations.[83,84] The lower value of the water self-diffusion coefficient found for the solution case would be consistent with the significant solvent structuring found in the structural analysis. The diffusion coefficient for the trehalose solute in TIP3P water was estimated to be approximately 0.9×10^{-5} cm^2 s^{-1}, essentially the same as was previously estimated for maltose from MD simulations.[28] Because there is only one solute molecule, the statistical error in the solute mean-square displacement data is much greater than for the solvent, and the numbers for both of these sugars must be considered to be rough estimates only.

IV. Conclusions

From the application of the present anisotropic density mapping procedures to the MD simulations of trehalose, it can be seen that this approach can be quite useful in mapping out the anisotropic structure imposed on solvent water by complex solutes. However, the procedure works best for relatively rigid solutes, and considerable information is lost when there is internal conformational flexibility. The procedure would apparently be difficult to apply to large solutes, since even the small conformational fluctuations of the fairly rigid trehalose resulted in the loss of considerable information. However, by judicious placement of the internal reference coordinate system, it is possible to map out the local solvent structuring around a particular portion of a larger oligomer or polymer, such as a single residue, as has been done for crystallographic data for amino acid side chains in different protein environments.[57]

(81) Tait, M. J.; Suggett, A.; Franks, F.; Ablett, S.; Quickenden, P. A. *J. Solution Chem.* **1972**, *1*, 131−151.
(82) Mashimo, S.; Miura, N.; Umehara, T. *J. Chem. Phys.* **1992**, *97*, 6759−6765.
(83) Sciortino, F.; Geiger, A.; Stanley, H. E. *Nature* **1991**, *354*, 218−221.
(84) Sciortino, F.; Geiger, A.; Stanley, H. E. *J. Chem. Phys.* **1992**, *96*, 3857−3865.

Protein side chains with multiple possible conformations and loops with alternate positions will make it difficult to map out their solvation shells with any precision. One possible approach to dealing with the problem of solute flexibility would be to keep the solute rigid in the simulation. This approximation might be acceptable for processes which are slow relative to the time required for solvent diffusion and reorganization, particularly in cases such as when the solute has more than one conformational state, spending the majority of its time in one or the other of the stable states and relatively little time converting between them. This situation might well apply to many of the cases of alternate side chain or loop positions.

In the application of these techniques to trehalose, it was found that trehalose imposes considerable structure on the adjacent water molecules. This structure is much more extensive than that found in pure liquid water, as in the cases of the monosaccharides previously studied. Also as was found with other sugars, this solvent structure appears to be a specific function of the chemical structure of the solute. A particularly interesting feature of the hydration of trehalose is the band of solvent density running around the middle of the molecule, centered on the glycosidic linkage and made up of water molecules interacting with both rings. However, none of the present results suggest a clear-cut reason why this sugar should be more effective in controlling adjacent water molecules than other sugars. In particular, the general hydration behavior observed in the present simulations does not differ dramatically from that of maltose or sucrose. It is possible that the small differences found in the simulations of these sugars are sufficient to account for their differing antidesiccant properties, but the mechanism remains unclear. It is also possible that the close similarity of the crystal hydrate structure to that in the simulations, with solvent water molecules preferentially occupying the same positions as the crystallographic water molecules, indicates that trehalose has a greater effect on its solvent. It could also be that the rather similar hydration behavior of these disaccharides is only indirectly relevant to their antidesiccant properties, as might be the case if the majority of the effect comes from direct binding of trehalose to membrane head groups, as has been suggested.[8] Perhaps the matter can be resolved through additional simulations, possibly including studies of sugars with only one full solvation shell or less, to examine the effects of lyophilization. It would also be quite interesting to perform simulations near or below the freezing point to determine if there is a significant restructuring of the solvent in that temperature regime as has been suggested by Batta et al.[17]

Acknowledgment. This work was supported by Grant No. CHE-9307690 (to J.W.B.) from the National Science Foundation.

JA970798V